nature communications

Article

https://doi.org/10.1038/s41467-025-67482-1

Decatungstate-photocatalyzed transfer hydrogenation of unsaturated compounds using alcohol as the hydrogen source

Received: 30 April 2025

Accepted: 2 December 2025

Published online: 06 January 2026

Check for updates

Teng Zhang[1], Zheng-Feng Zhang[2], Xuan Lan[3], Si-Yi Li[3], Ming-Der Su[2,4] ✉, Yonggui Robin Chi[1] ✉, Lixin Wu[5] & Cheuk-Wai So[1] ✉

We present a simple and efficient photocatalytic method for the transfer hydrogenation of unsaturated compounds using alcohol as the hydrogen source and low-cost decatungstate as the photocatalyst. Our approach operates under mild and ambient conditions and demonstrates broad substrate compatibility, including alkyl, aryl, and heteroatom-substituted alkenes, alkynes, azo compounds and nitroarenes. To our knowledge, this study represents the first instance of using tungsten-based catalysts for the photocatalytic transfer hydrogenation of unsaturated compounds. Notably, the catalytic system, employing decatungstate as the catalyst and alcohol as the hydrogen source, exhibits high chemoselectivity, enabling selective hydrogenation of alkenes and alkynes even in the presence of reactive groups like ketones and carboxylic acids. These features highlight the considerable potential of this approach for practical and sustainable applications in organic synthesis.

Hydrogenation of alkenes is one of the most fundamental transformations in organic synthesis, typically requiring both a catalyst and a hydrogen source[1–19]. The most common hydrogen source is hydrogen gas (H_2), known for its 100% atom efficiency. However, safety concerns related to handling flammable and potentially explosive H_2 have led to the exploration of alternative hydrogen sources[20–38].

Photochemistry offers a novel approach for converting organic substrates into alternative hydrogen sources. One notable strategy involves photocatalytic reduction of alkenes to radical anions, which subsequently react with Brønsted-Lowry acids or solvents as proton donors to facilitate catalytic hydrogenation[39]. For instance, Guo and Houk et al. employed the strong acid TfOH and thioxanthone (TX) to photo-catalytically reduce α,β-unsaturated carbonyl compounds by using *p*-xylene (solvent) as the proton source (Fig. 1a)[40]. Similarly, Polyzos et al. described an iridium-catalyzed reduction of alkenes, followed by a reaction with Brønsted-Lowry acids to produce alkanes (Fig. 1b)[41]. However, this technique is limited by the reduction potential of the targeted alkenes. An alternative strategy was then developed, where iridium complexes were usually used to photo-catalytically generate radical cations to undergo hydrogen atom transfer (HAT) reactions with alkenes to form hydrogen-adduct carbon radicals. This is followed by either protonation with a proton source or addition with a hydrogen radical source to achieve catalytic hydrogenation[42–46]. For example, Wenger et al. demonstrated that an iridium photocatalyst mediated the HAT reaction between triethylamine (TEA) and alkenes, with subsequent radical addition completing alkene hydrogenation (Fig. 1c)[45]. Moreover, Studer and coworkers developed an iridium-catalyzed system for generating phosphine radical cations that activated water molecules to form a PR_3–H_2O radical cation intermediate, effectively utilizing both hydrogen atoms from H_2O in the alkene hydrogenation through sequential heterolytic (H^+) and homolytic (H•) O–H bond cleavages (Fig. 1d)[46]. Despite these advancements, replacing these rare and costly iridium photocatalysts with more abundant and

[1]School of Chemistry, Chemical Engineering and Biotechnology, Nanyang Technological University, Singapore, Singapore. [2]Department of Applied Chemistry, National Chiayi University, Chiayi, Taiwan. [3]College of Chemistry and Materials Science, Zhejiang Normal University, Jinhua, China. [4]Department of Medicinal and Applied Chemistry, Kaohsiung Medical University, Kaohsiung, Taiwan. [5]State Key Laboratory of Supramolecular Structure and Materials and College of Chemistry, Jilin University, Changchun, China. ✉e-mail: midesu@mail.ncyu.edu.tw; robinchi@ntu.edu.sg; CWSo@ntu.edu.sg

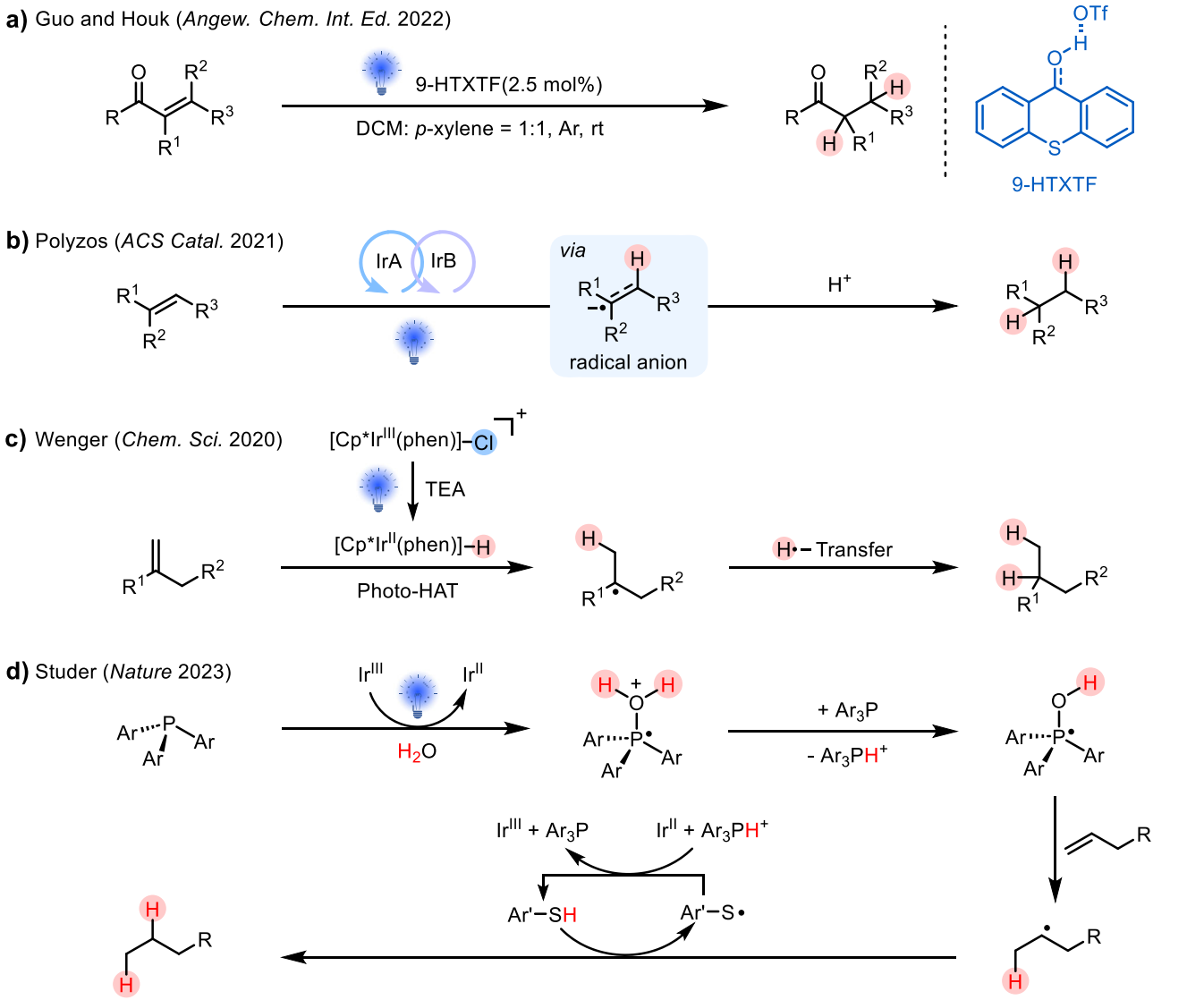

Fig. 1 | The previous work on photocatalytic transfer hydrogenation reactions. Strategies involve (**a**, **b**) photocatalytic reduction of alkenes and (**c**, **d**) hydrogen atom transfer (HAT) reactions with alkenes.

inexpensive alternatives would significantly enhance the sustainability of hydrogenation processes.

Alcohol is earth-abundant and sustainable, which would be a good candidate as a transfer hydrogenation reagent. However, the main difficulty for its use in the hydrogenation of alkenes originates from challenging homolytic cleavage of O–H and α-C–H bonds due to their high bond dissociation energies (BDE = *ca* 100 kcal/mol)[47]. This is supported by currently reported photocatalysts, which solely mediate homolytic cleavage of the α-C–H bond in alcohols, generating reactive nucleophilic α-C-centered radicals (•CR_2OH) for conjugate additions with Michael acceptors (Fig. 2)[48–53]. We propose that if the homolytic cleavage of the α-C(sp^3)–H bond of alcohol [$R_2C(H)OH$] generates a hydrogen radical (H•) and a relatively stable alcohol radical (•CR_2OH), this alcohol radical could undergo O–H bond cleavage, rather than reacting with the alkene, producing a C = O double bond in aldehydes or ketones ($R_2C=O$) and a second H•. These two hydrogen radicals could readily add across the C = C double bond, enabling effective alkene hydrogenation (Fig. 2).

Transition metal-polyoxometalate hybrid clusters demonstrate good activity in mediating direct hydrogenation[54–56], prompting us to explore whether a low-cost and earth-abundant decatungstate anion, $[W_{10}O_{32}]^{4-}$ alone can be used as a photocatalyst for transfer hydrogenation. Upon irradiation, the decatungstate anion is excited to a reactive state capable of abstracting α-H atoms from alcohols, generating alcohol radicals (•CR_2OH) and reduced decatungstate species, $H^+[W_{10}O_{32}]^{5-}$. The alcohol radical undergoes homolytic cleavage of the O–H bond, forming an aldehyde or ketone and a hydrogen radical (H•). This hydrogen radical then reacts with the C = C double bond of an alkene ($R_2C=CR_2$), producing a carbon-centered radical ($R_2(H)–C(•)R_2$). The photocatalytic cycle is completed when this alkyl radical undergoes HAT with $H^+[W_{10}O_{32}]^{5-}$, yielding the hydrogenated alkene [$R_2(H)–C(H)R_2$] and regenerating the decatungstate anion $[W_{10}O_{32}]^{4-}$. Herein, we report a simple, mild, and efficient strategy for unsaturated compounds hydrogenation using alcohol as the hydrogen source and low-cost decatungstate as the photocatalyst. To our knowledge, this study represents the first instance of using tungsten-based catalysts for the transfer hydrogenation of unsaturated compounds. Notably, the decatungstate/alcohol catalytic system exhibits excellent chemoselectivity, enabling selective hydrogenation of alkenes and alkynes even in the presence of reactive groups like ketones and carboxylic acids. These features highlight the significant potential of this approach for practical and sustainable applications in organic synthesis.

https://doi.org/10.1038/s41467-025-67482-1

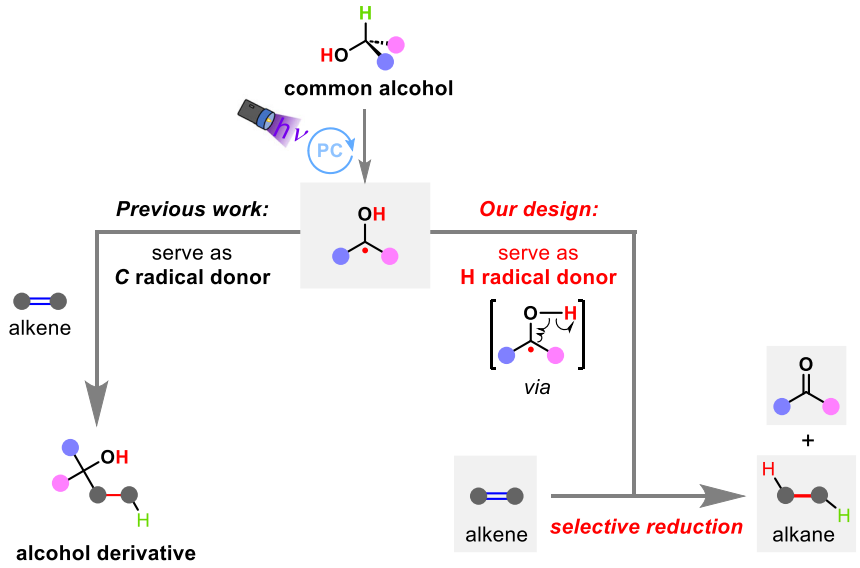

Fig. 2 | The designed photocatalytic transfer hydrogenation of alkenes using alcohol as the hydrogen source. Previous work involves alcohol radicals as C-radical donor, whereas our work involves alcohol radicals as H radical donor.

Results

Catalysis and Substrate Scope

We initially investigated prenol **2a**, a natural alcohol derived from biomass, as a hydrogen source for the transfer hydrogenation of 1,2-dibenzoylethylene (**1a**) (Fig. 3a). It is because the prenol-derived α-C radical ($Me_2C=CHCH(•)OH$) formed during α-C(sp^3)–H bond activation can be stabilized by delocalization with the C = C double bond[57–59]. This stabilization likely reduces the reactivity of the radical toward **5a**, thereby enabling the homolytic cleavage of the O–H bond to proceed efficiently. Upon 390 nm LED irradiation and with 5 mol% TBADT (tetrabutylammonium decatungstate) as the photocatalyst, the reaction yielded four types of products: the hydrogenated compound **4a** (isolated yield: 86%), aldehyde **3a**, α-C(sp^3)–H bond addition compound **5a** (isolated yield: 5%), and a mixture of dimeric by-products arising from coupling of C = C double bond (Figure S3 for their X-ray crystal structure). When TBADT was replaced with 2,4,6-triphenylpyrylium, a lower yield of compound **4a** was observed. In contrast, using anthraquinone as a photocatalyst led to the formation of compound **5a** (67%) as the major product. These findings speculate that the stability of the reduced photocatalyst, H^+[photocatalyst]$^-$, plays a key role in determining whether the prenol-derived α-C radical ($Me_2C=CHCH(•)OH$) is capable of undergoing rearrangement to form **3a** and H• before the HAT step by H^+[photocatalyst]$^-$ occurs. The use of EosinY as a photocatalyst resulted in a mixture of dimeric by-products as major products, while **4a** and **5a** are minor products. EosinY was capable of photocatalytic C–H bond addition of 2-benzylidenemalononitrile with simple alcohols in quantitative conversion[49]. As such, we replaced compound **1a** with 2-benzylidenemalononitrile, where EosinY catalyzed hydrogenation of 2-benzylidenemalononitrile with **2a** to form [$PhCH_2CH(CN)_2$] in 21% yield, along with a C–H bond addition product in 73% yield (see the Supplementary Information Section 3 for details). This supports our abovementioned hypothesis that prenol-derived α-C radical ($Me_2C=CHCH(•)OH$) has relatively higher stability, which allows hydrogenation to occur, even EosinY prefers to mediate C–H bond addition.

Next, we evaluate the performance of primary and secondary alcohols in the TBADT-catalyzed transfer hydrogenation of 1,2-dibenzoylethylene (Fig. 3b). Prenol is the most effective, yielding **4a** with the highest isolated yield. Allyl alcohol (**2b**) also performed well, producing **4a** in 79% isolated yield, while natural alcohol geraniol (**2c**) afforded a comparable yield of 81%. Benzyl alcohol (**2d**) and pyridin-2-ylmethanol (**2e**) were efficient hydrogen donors, delivering isolated yields of 72% and 76%, respectively. Secondary alcohols such as 1-phenylethanol (**2f**) and 1-(pyridin-4-yl)ethan-1-ol (**2g**) achieved similarly high isolated yields (75% and 86%, respectively). Furan-2-ylmethanol (**2h**) is cumbersome in the catalysis based on the moderate isolated yield of **4a** (48%). Conversely, simple alcohols such as ethanol (**2i**) and 2-propanol (**2j**) produced lower isolated yields of **4a** (26% and 29%). These findings show that the nucleophilic alcohol α-C-centered radicals ($•CR_2OH$) contain an unsaturated moiety (R= benzene, pyridine or alkene), having high efficiency in the hydrogenation of alkene, probably due to the stabilization of the radical, allowing homolytic O–H bond cleavage. Overall, these results demonstrate the feasibility of using a diverse array of primary and secondary alcohols as hydrogen sources in TBADT-mediated transfer hydrogenation, emphasizing the robustness and versatility of this approach.

With optimized reaction conditions established, we explored the substrate scope of olefins, as summarized in Fig. 4. The hydrogenation of 1,2-dibenzoylethylene (**1a**) with prenol produced **4a** in an excellent isolated yield (86%). Encouraged by this result, we explored α,β-unsaturated carbonyl compounds. To our delight, the 4-phenyl-3-buten-2-one (**1b**) reacted efficiently to produce 4-phenylbutan-2-one (**4b**) in 76% isolated yield. Derivatives of **1b** with electron-donating and electron-withdrawing substituents at different positions *ortho*- (**1c,** *o*-Me; **1d,** *o*-F), *meta*- (**1e,** *m*-OMe), and *para*- (**1f,** *p*-OMe; **1g,** *p*-OH; **1h,** *p*-Cl; **1i,** *p*-F; **1j,** *p*-CF_3) were successfully hydrogenated, yielding the corresponding products (**4c**-**4j**) in moderate to high isolated yields (54-85%). The results revealed that the electron-rich substituents at the β position (**1c, 1e, 1f, 1g**) led to slightly reduced isolated yields (54–63%). Replacing the phenyl group with a methyl (**1k**) or α-naphthyl substituent (**1l**) did not significantly affect product yields, producing **4k** and **4l** in 66% and 71% isolated yields, respectively. However, the hydrogenation of **1m**, which contains a pyridine substituent, led to reductive coupling instead of hydrogenation to form **6m** in 91% isolated yield. Moreover, 1-phenylbuten-1-one (**1n**) and 1,3-diphenylpropen-1-one (**1o**) were hydrogenated, giving a moderate isolated yield of 41% and 32%, respectively. Carboxylic acid and ester substituents enhanced reactivity, yielding **4p**-**4s** in 67-87% isolated yields. Importantly, gram-scale hydrogenation of **1s** (1.589 g, 7.4 mmol) afforded **4s** in 82% yield (1.251 g), underscoring the robustness and practicality of this catalytic protocol for larger-scale synthesis. Terminal olefins, namely 3-buten-2-one (**1t**) and 1-phenylprop-2-en-1-one (**1u**) were effectively hydrogenated leading to **4t** (86%) and **4u**

https://doi.org/10.1038/s41467-025-67482-1

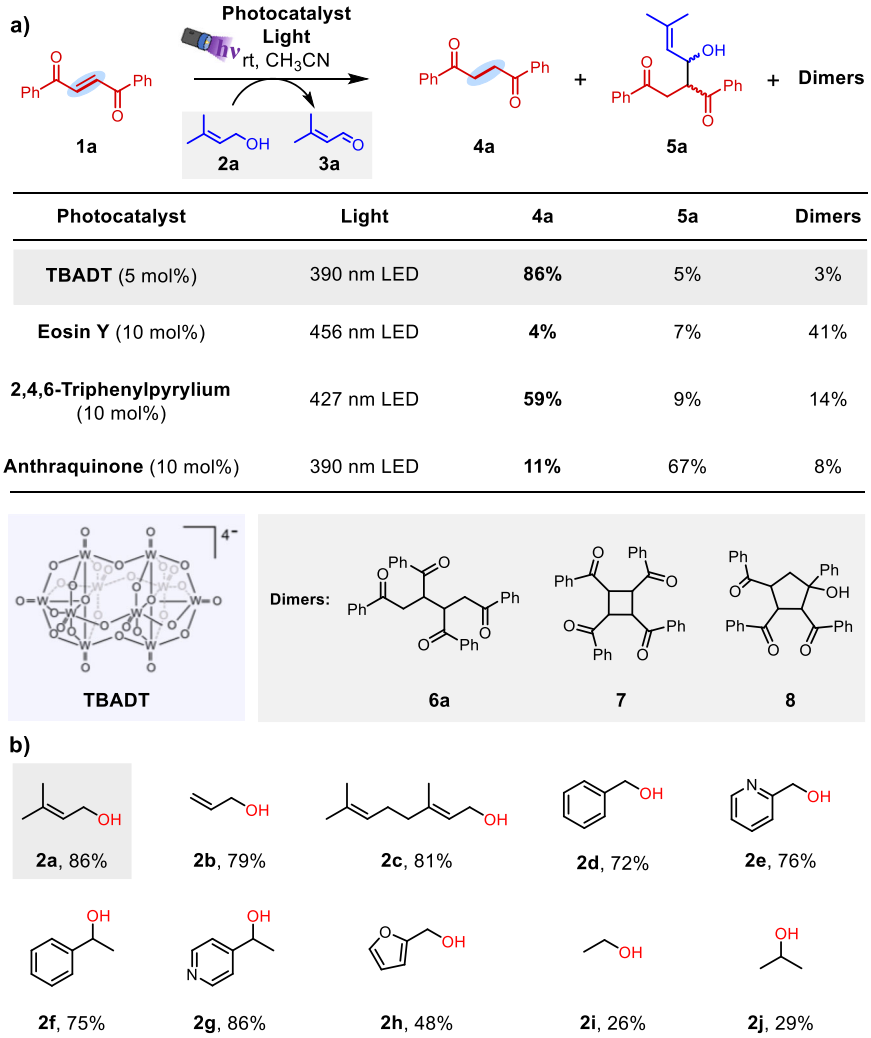

Photocatalyst	Light	4a	5a	Dimers
TBADT (5 mol%)	390 nm LED	**86%**	5%	3%
Eosin Y (10 mol%)	456 nm LED	**4%**	7%	41%
2,4,6-Triphenylpyrylium (10 mol%)	427 nm LED	**59%**	9%	14%
Anthraquinone (10 mol%)	390 nm LED	**11%**	67%	8%

Fig. 3 | Optimization of reaction conditions. a Photosensitizers catalyzed hydrogenation of 1,2-dibenzoylethylene **1a** with prenol **2a** as the hydrogen source. The yields of the target product **4a** are highlighted in bold corresponding to the photocatalysts examined. The optimized result is indicated. **b** Scope of alcohols used for the formation of the target product **4a**. Reaction conditions: olefin (0.1 mmol), alcohol (5 equiv.), CH_3CN (2 mL), TBADT (5 mol%), 390 nm LEDs (40 W), 6 h reaction time, room temperature. Yields of **4a** are isolated yields. The highest yield of **4a** resulting from the use of **2a** as the alcohol source is indicated.

(84%) in good isolated yields, respectively. When more substituted terminal olefin, namely, 3-methylbut-3-en-2-one (**1v**) was hydrogenated, the isolated yield of **4v** dropped to 64%. Cycloenone **1w** and more substituted derivative **1x** also reacted to form cyclohexanones **4w** (76%) and **4x** (43%), respectively. Next, reactive functional groups namely ester, nitro, and cyano groups in **1y**-**1aa** were well compatible in catalysis (38-46%). The 1,1-disubstituted olefins with electron-withdrawing substituents were well compatible in catalysis (**1ab**, 43%), however, those with electron-donating groups were not tolerated. Pyridine substituent promoted the hydrogenation, where 1,2-di(4-pyridyl)ethylene (**1ac**) was converted into **4ac** with an excellent isolated yield of 94%. Remarkably, the anti-lymphoma and leukemia cancer drug, namely Ibrutinib (**1ad**) was hydrogenated to produce **4ad** in 56% isolated yield, demonstrating the utility of this catalytic method in the late-stage functionalization of pharmaceutical agents.

Subsequently, we investigated the hydrogenation of other types of unsaturated bonds. N = N double bonds encompassing both symmetrical and asymmetrical azo compounds (**1ae-1al**) were efficiently reduced under the optimized conditions, yielding **4ae-4al** in good isolated yields (82–89%). It appears that the N lone pair of electrons does not affect the reaction mechanism. Phenylacetylene and its derivatives with various substituents (**9a**-**9h**) were efficiently converted to the corresponding terminal olefins (**10a**-**10h**) in 61-91% isolated yields. Furthermore, 4-phenyl-1-butyne and alkyl alkynes (**9i**-**9l**) gave hydrogenated products (**10i**-**10l**) in 73–83% yields, demonstrating compatibility beyond aromatic substrates. Alkynes bearing carbonyl substituents (**9a, 9b, 9t**, and **9u**) underwent double hydrogenation to directly form alkanes (**4a**-**4u**, 69-83% isolated yields). The reduction proceeds in a stepwise manner: initial hydrogenation affords electron-deficient olefins (**1a, 1b, 1t**, and **1u**), which remain highly reactive due to the strong activating effect exerted by the carbonyl groups. As a consequence, these olefins serve as transient intermediates and promptly undergo further hydrogenation under the catalytic conditions, ultimately affording the fully reduced alkane products.

In addition, we explored the hydrogenation of a variety of nitroarenes (**12a-12i**, Fig. 5). All substrates were efficiently reduced, affording the corresponding amines in good yields (61–83%). Notably, the antiparasitic drug Niclosamide (**11h**) and the calcium channel antagonist *p*-Nifedipine (**11i**) were successfully hydrogenated to **12h** and **12i** in 73% and 79% isolated yield, respectively. These results highlight the practicality of our method for the late-stage functionalization of pharmaceutically relevant molecules.

Mechanistic Investigations

To clarify the catalytic mechanism, deuterated benzyl alcohols $PhCH_2OD$ and $PhCD_2OH$ were reacted with **1ac** (Fig. 6a). These

https://doi.org/10.1038/s41467-025-67482-1

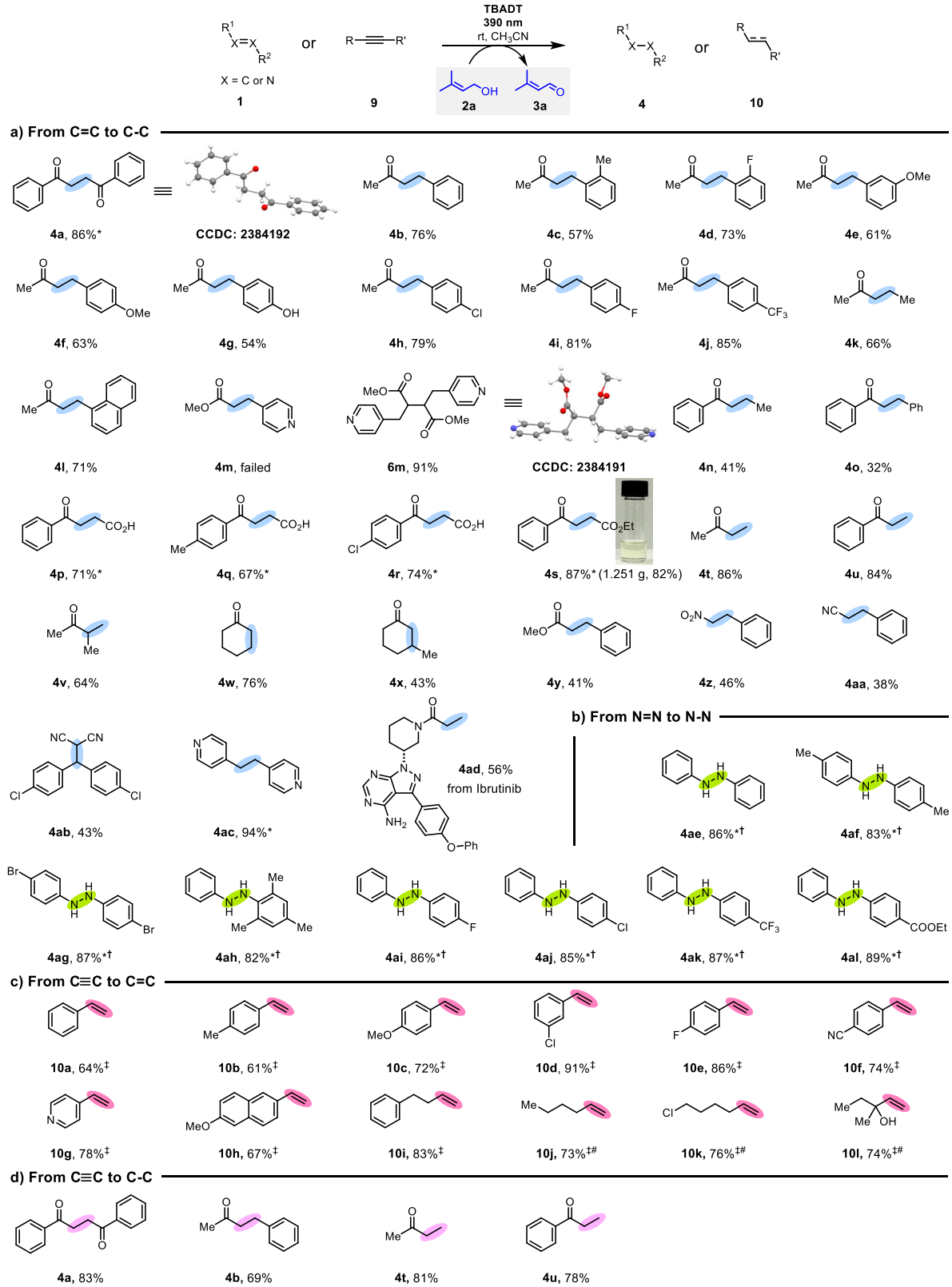

Fig. 4 | TBADT photocatalyzed hydrogenation of unsaturated organic compounds with prenol as the hydrogen source. Reaction conditions: substrate **a** alkenes, **b** diazo compounds, **c**, **d** alkynes (0.1 mmol), prenol (5 equiv.), CH_3CN (2 mL), TBADT (5 mol%), 390 nm LEDs (40 W), 24 h, room temperature; yields are isolated yields. *6 h reaction time. †400 nm LEDs (40 W). ‡Reaction at 70 °C. #Yields determined from crude ^1H NMR spectra using 1,3,5-trimethoxybenzene as the internal standard.

https://doi.org/10.1038/s41467-025-67482-1

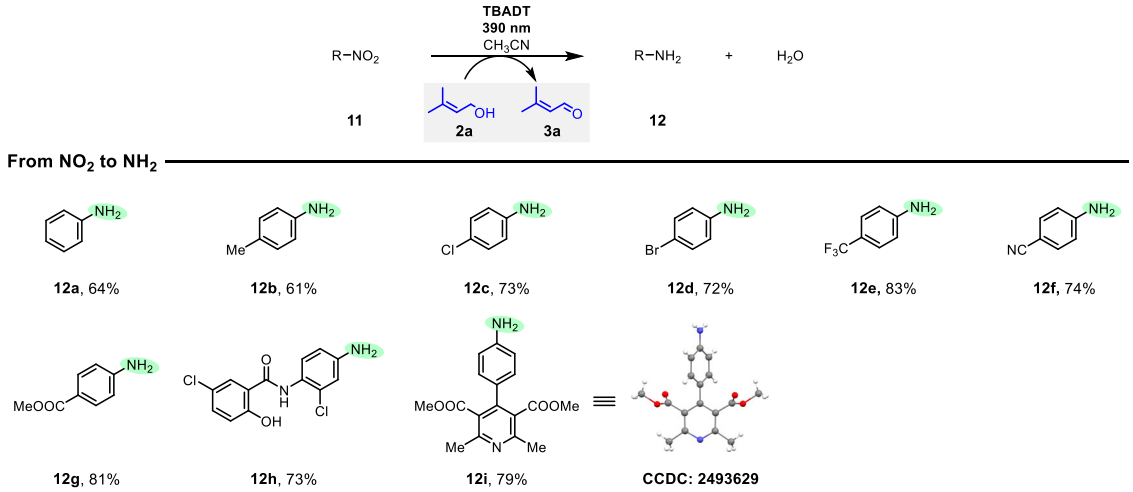

Fig. 5 | TBADT photocatalyzed hydrogenation of nitroarenes with prenol as the hydrogen source. Reaction conditions: nitroarene (0.1 mmol), prenol (5 equiv.), CH_3CN (2 mL), TBADT (5 mol%), 390 nm LEDs (40 W), 70 °C, 12 h; all yields are isolated yields.

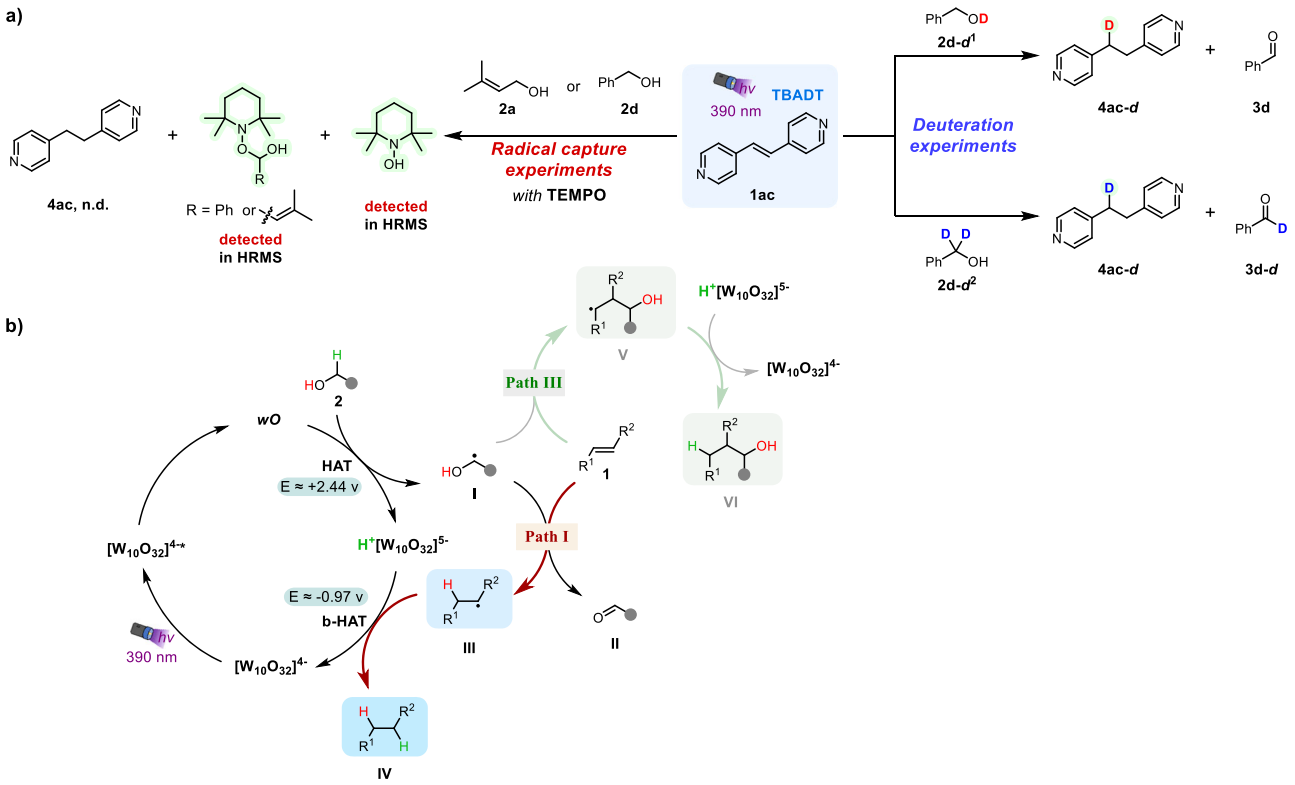

Fig. 6 | Experimental mechanistic studies. a Deuteration and radical capture experiments; **b** proposed mechanism for the transfer hydrogenation of alkenes.

reactions resulted in a 1:1 molar ratio of **4ac-*d*** and **3d**, and a 1:1 molar ratio of **4ac-*d*** and **3d-*d***, respectively (Figs. S7 and S8), confirming that alcohols are the sole hydrogen source. Moreover, introducing the radical scavenger TEMPO (1 equiv.) significantly inhibited the formation of **4ac** as the H• and alcohol α-C centered radicals were quenched by TEMPO (Figs. S10 and S11 showing the presence of the quenched radicals in HRMS). These findings indicate that the mechanism involves the activation of the α-C(sp^3)–H bond of alcohols to form alcohol α-C-centered radicals in the first step. To further understand why the alcohol α-C-centered radical undergoes O–H bond cleavage rather than directly adding to the alkene during catalysis, density functional theory (DFT) calculations were performed using butenone **1t** and prenol α-C-centered radical **R2a** as model substrates. Three potential hydrogenation pathways were explored.

In **Path I** (Fig. 7), the **R2a** undergoes homolytic cleavage of its O–H bond and addition of H• at the *β*-position of **1t** via **TS-A** ($\Delta G^{\ddagger}$ = 23.3 kcal/mol) to form intermediate **A** and **3a** (ΔG = −8.3 kcal/mol). In contrast, the addition of H• at the *α*-position of **1t** is infeasible due to the high kinetic barrier (**Path II, TS-B**: $\Delta G^{\ddagger}$ = 43.8 kcal/mol, see Fig. S16 in Supplementary Information). Intermediate **A** then undergoes HAT with $H^+[W_{10}O_{32}]^{5-}$ via **TS-A2** ($\Delta G^{\ddagger}$ = 23.3 kcal/mol) to form **4t**·$[W_{10}O_{32}]^{4-}$ complex **Prod-A2** (ΔG = −76.9 kcal/mol). **4t** is then dissociated from $[W_{10}O_{32}]^{4-}$ to complete a catalytic cycle (ΔG = −66.3 kcal/mol). Finally, **Path I** is exergonic by 66.3 kcal/mol.

In the C–C bond formation pathway (**Path III**, Fig. 7), **R2a** adds to **1t** via **TS-C** (ΔG = 13.6 kcal/mol), forming intermediate **C** (ΔG = −5.8 kcal/mol). It then undergoes HAT with $H^+[W_{10}O_{32}]^{5-}$ via **TS-C2** ($\Delta G^{\ddagger}$ = −67.8 kcal/mol) to form [MeC(O)CH_2CH_2CH(OH)

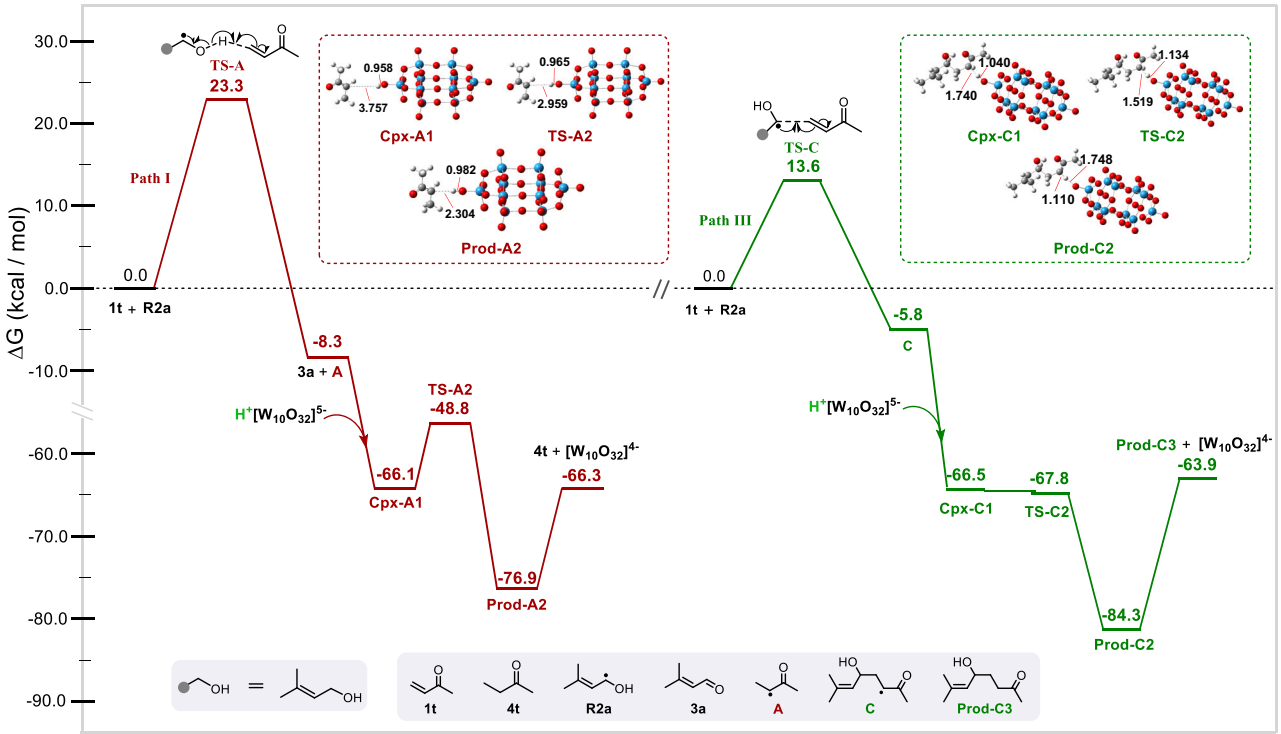

Fig. 7 | Reaction mechanism studied by DFT calculations. Calculated Gibbs free energy profile (kcal/mol) illustrating the reaction pathways of the prenol radical in hydrogenation Path I (red) and α-C(sp^3)–H functionalization with butanone Path III (green).

$CH=C(Me)_2]$•$[W_{10}O_{32}]^{4-}$ complex **Prod-C2** (ΔG = −84.3 kcal/mol). However, the C–H bond addition product $[MeC(O)CH_2CH_2CH(OH)CH=C(Me)_2]$ (**Prod-C3**) requires a higher activation barrier of 20.4 kcal/mol to dissociate from $[W_{10}O_{32}]^{4-}$ to complete the catalytic cycle (ΔG = −63.9 kcal/mol). Finally, Path **III** is exergonic by 63.9 kcal/mol. Overall, these results indicate that the catalytic system preferentially follows the hydrogenation pathway (**Path I**) rather than the α-C(sp^3)–H functionalization pathway (**Path III**).

Based on the experimental data and DFT calculations, a plausible mechanism for decatungstate-photocatalyzed transfer hydrogenation of alkenes using alcohol as the hydrogen source is proposed (Fig. 6b). Upon 390 nm LED light irradiation, decatungstate is excited to $[W_{10}O_{32}]^{4-*}$, and rapidly relaxes to its reactive state ***w*O**[60,61]. This ***w*O** species initiates the process by abstracting an α-hydrogen atom from alcohol to produce an α-carbon-centered alcohol radical (•CROH **I**)[62–64] and $H^+[W_{10}O_{32}]^{5-}$, due to the high redox potential of ***w*O**/$[W_{10}O_{32}]^{5-}$ (E = +2.44 V vs SCE)[65]. The resulting radical undergoes first hydrogen atom transfer (**Path I**) to alkene, forming a radical intermediate **III** and aldehyde/ketone (**II**). The intermediate **III** subsequently undergoes a back-HAT with $H^+[W_{10}O_{32}]^{5-}$, producing the final alkane product (**IV**) and regenerating the starting catalyst $[W_{10}O_{32}]^{4-}$ to close the catalytic cycle. In addition, the alcohol radical •CROH (**I**) can undergo conjugate addition with alkenes via **Path III** to generate intermediate **V**, which reacts with $H^+[W_{10}O_{32}]^{5-}$ to yield a byproduct **VI**.

In summary, we have developed a simple, mild, and efficient photocatalytic method for the transfer hydrogenation of unsaturated compounds using alcohols as the hydrogen source and low-cost decatungstate as the photocatalyst. This method demonstrates broad substrate compatibility, high chemoselectivity, and practicality under ambient conditions. Mechanistic studies reveal that the hydrogenation proceeds via a radical-mediated pathway involving the sequential homolytic cleavage of α-C(sp^3)–H and O–H bonds in alcohols. DFT calculations further confirmed that the hydrogenation pathway is more exergonic than the side α-C(sp^3)–H functionalization route, indicating it is thermodynamically favored, consistent with experimental observations. These findings highlight the significant potential of the decatungstate/alcohol catalytic system in practical organic synthesis, offering a sustainable approach for unsaturated compounds hydrogenation.

Methods

General procedures for transfer hydrogenation of unsaturated compounds

In a glovebox, unsaturated compounds (0.1 mmol), TBADT (5 mol%), prenol (0.5 mmol, 5 equiv.), and anhydrous acetonitrile (2 mL) were placed in a 10 mL Schlenk tube equipped with a magnetic stir bar. The reaction mixture was subsequently irradiated with an LED light (Kessil 40 W) at room temperature (unless otherwise noted) for 6–24 h, with 24 h being sufficient for all substrates. Then, the solvent was removed under reduced pressure using a rotary evaporator, and the resulting residue was purified by silica gel column chromatography. The appropriate eluent system (hexane, hexane/ethyl acetate, DCM/methanol or ethyl acetate/methanol) was selected based on the polarity of the target product, yielding the corresponding products For the detailed experimental methods described in this manuscript, please refer to the Supplementary Information.

Data availability

All data generated or analyzed during this study are available within the article and its Supplementary Information files, or from the corresponding author upon request. Details about materials and methods, experimental procedures, characterization data, NMR spectra and DFT calculations are available in the Supplementary Information. The optimized Cartesian coordinates are provided in the Source Data file. CCDC-2384191 (for **6 m**), 2384192 (for **4a**), 2402528-2402530 (for **6a, 7** and **8**), and 2493629 (for **12i**), contain the supplementary crystallographic data for this paper. These data are provided free of charge by the joint Cambridge Crystallographic Data Centre and Fachinformationszentrum Karlsruhe Access Structures service. Source data are provided with this paper.

References

1. Verendel, J. J., Pàmies, O., Diéguez, M. & Andersson, P. G. Asymmetric Hydrogenation of Olefins Using Chiral Crabtree-type Catalysts: Scope and Limitations. *Chem. Rev.* **114**, 2130–2169 (2014).
2. Wang, D.-S., Chen, Q.-A., Lu, S.-M. & Zhou, Y.-G. Asymmetric Hydrogenation of Heteroarenes and Arenes. *Chem. Rev.* **112**, 2557–2590 (2012).
3. Qu, R., Junge, K. & Beller, M. Hydrogenation of Carboxylic Acids, Esters, and Related Compounds over Heterogeneous Catalysts: A Step toward Sustainable and Carbon-Neutral Processes. *Chem. Rev.* **123**, 1103–1165 (2023).
4. Cabré, A., Verdaguer, X. & Riera, A. Recent Advances in the Enantioselective Synthesis of Chiral Amines via Transition Metal-Catalyzed Asymmetric Hydrogenation. *Chem. Rev.* **122**, 269–339 (2022).
5. Wen, J., Wang, F. & Zhang, X. Asymmetric Hydrogenation Catalyzed by First-row Transition Metal Complexes. *Chem. Soc. Rev.* **50**, 3211–3237 (2021).
6. Lückemeier, L., Pierau, M. & Glorius, F. Asymmetric arene hydrogenation: towards sustainability and application. *Chem. Soc. Rev.* **52**, 4996–5012 (2023).
7. Kumar, A., Daw, P. & Milstein, D. Homogeneous Catalysis for Sustainable Energy: Hydrogen and Methanol Economies, Fuels from Biomass, and Related Topics. *Chem. Rev.* **122**, 385–441 (2022).
8. Lam, J., Szkop, K., Mosaferi, E. & Stephan, D. W. FLP Catalysis: Main Group Hydrogenations of Organic Unsaturated Substrates. *Chem. Soc. Rev.* **48**, 3592–3612 (2019).
9. Kraft, S., Ryan, K. & Kargbo, R. B. Recent Advances in Asymmetric Hydrogenation of Tetrasubstituted Olefins. *J. Am. Chem. Soc.* **139**, 11630–11641 (2017).
10. Ding, Z. et al. Ru-Catalyzed Asymmetric Hydrogenation of α,β-Unsaturated γ-Lactams. *J. Am. Chem. Soc.* **146**, 25312–25320 (2024).
11. Friedfeld, M. R., Zhong, H., Ruck, R. T., Shevlin, M. & Chirik, P. J. Cobalt-catalyzed asymmetric hydrogenation of enamides enabled by single-electron reduction. *Science* **360**, 888–893 (2018).
12. Margarita, C. & Andersson, P. G. Evolution and Prospects of the Asymmetric Hydrogenation of Unfunctionalized Olefins. *J. Am. Chem. Soc.* **139**, 1346–1356 (2017).
13. Davies, A. T., Pickett, P. M., Slawin, A. M. Z. & Smith, A. D. Asymmetric Synthesis of Tri- and Tetrasubstituted Trifluoromethyl Dihydropyranones from α-Aroyloxyaldehydes via NHC Redox Catalysis. *ACS Catal* **4**, 2696–2700 (2014).
14. Kim, A. N. & Stoltz, B. M. Recent Advances in Homogeneous Catalysts for the Asymmetric Hydrogenation of Heteroarenes. *ACS Catal* **10**, 13834–13851 (2020).
15. Wei, H. et al. Enantioselective Synthesis of Chiral β^2-Amino Phosphorus Derivatives via Nickel-Catalyzed Asymmetric Hydrogenation. *J. Am. Chem. Soc.* **147**, 342–352 (2025).
16. Mas-Roselló, J., Smejkal, T. & Cramer, N. Iridium-catalyzed acid-assisted asymmetric hydrogenation of oximes to hydroxylamines. *Science* **368**, 1098–1102 (2020).
17. Yang, F., Xie, J.-H. & Zhou, Q.-L. Highly Efficient Asymmetric Hydrogenation Catalyzed by Iridium Complexes with Tridentate Chiral Spiro Aminophosphine Ligands. *Acc. Chem. Res.* **56**, 332–349 (2023).
18. Chakrabortty, S. et al. Cobalt-Catalyzed Enantioselective Hydrogenation of Trisubstituted Carbocyclic Olefins: An Access to Chiral Cyclic Amides. *Angew. Chem. Int. Ed.* **62**, e202301329 (2023).
19. Wiesenfeldt, M. P., Nairoukh, Z., Li, W. & Glorius, F. Hydrogenation of Fluoroarenes: Direct Access to All-cis-(multi)-fluorinated Cycloalkanes. *Science* **357**, 908–912 (2017).
20. Wang, D. & Astruc, D. The Golden Age of Transfer Hydrogenation. *Chem. Rev.* **115**, 6621–6686 (2015).
21. Santana, C. G. & Krische, M. J. From Hydrogenation to Transfer Hydrogenation to Hydrogen Auto-Transfer in Enantioselective Metal-Catalyzed Carbonyl Reductive Coupling: Past, Present, and Future. *ACS Catal* **11**, 5572–5585 (2021).
22. Pang, M. et al. Controlled Partial Transfer Hydrogenation of Quinolines by Cobalt-Amido Cooperative Catalysis. *Nat. Commun.* **11**, 1249 (2020).
23. Lau, S., Gasperini, D. & Webster, R. L. Amine-Boranes as Transfer Hydrogenation and Hydrogenation Reagents: A Mechanistic Perspective. *Angew. Chem. Int. Ed.* **60**, 14272–14294 (2021).
24. Zhou, Q., Meng, W., Yang, J. & Du, H. A Continuously Regenerable Chiral Ammonia Borane for Asymmetric Transfer Hydrogenations. *Angew. Chem. Int. Ed.* **57**, 12111–12115 (2018).
25. Cummings, S. P., Le, T.-N., Fernandez, G. E., Quiambao, L. G. & Stokes, B. J. Tetrahydroxydiboron-Mediated Palladium-Catalyzed Transfer Hydrogenation and Deuteriation of Alkenes and Alkynes Using Water as the Stoichiometric H or D Atom Donor. *J. Am. Chem. Soc.* **138**, 6107–6110 (2016).
26. Xu, H., Yang, P., Chuanprasit, P., Hirao, H. & Zhou, J. S. Nickel-Catalyzed asymmetric transfer hydrogenation of hydrazones and other ketimines. *Angew. Chem. Int. Ed.* **54**, 5112–5116 (2015).
27. Zhao, E. et al. Transfer Hydrogenation with a Carbon-Nitride-Supported Palladium Single-Atom Photocatalyst and Water as a Proton Source. *Angew. Chem. Int. Ed.* **61**, e202207410 (2022).
28. Sun, Y. et al. Hydrogen bond enhanced enantioselectivity in the Nickel-catalyzed transfer hydrogenation of α-substituted acrylic acid with formic acid. *ACS Catal* **13**, 14213–14220 (2023).
29. Broggi, J. et al. The Isolation of [Pd{OC(O)H}(H)(NHC)(PR_3)] (NHC = N-Heterocyclic Carbene) and Its Role in Alkene and Alkyne Reductions Using Formic Acid. *J. Am. Chem. Soc.* **135**, 4588–4591 (2013).
30. Wang, F. et al. Asymmetric Transfer Hydrogenation of α-Substituted-β-Keto Carbonitriles via Dynamic Kinetic Resolution. *J. Am. Chem. Soc.* **143**, 2477–2483 (2021).
31. Lin, Y., Xu, G. & Tang, W. Chiral Polymeric Diamine Ligands for Iridium-Catalyzed Asymmetric Transfer Hydrogenation. *J. Am. Chem. Soc.* **146**, 27736–27744 (2024).
32. Wu, J. et al. Synthesis of Chiral Piperidines from Pyridinium Salts via Rhodium-Catalysed Transfer Hydrogenation. *Nat. Catal.* **5**, 982–992 (2022).
33. Lan, S. et al. Asymmetric Transfer Hydrogenation of Cyclobutenediones. *J. Am. Chem. Soc.* **146**, 4942–4957 (2024).
34. Kattamuri, P. V. & West, J. G. Hydrogenation of Alkenes via Cooperative Hydrogen Atom Transfer. *J. Am. Chem. Soc.* **142**, 19316–19326 (2020).
35. Liu, X. et al. Enable Biomass-Derived Alcohols Mediated Alkylation and Transfer Hydrogenation. *Nat. Commun.* **15**, 7012 (2024).
36. Luo, G.-G. et al. Total Structure, Electronic Structure and Catalytic Hydrogenation Activity of Metal-Deficient Chiral Polyhydride Cu57 Nanoclusters. *Angew. Chem. Int. Ed.* **62**, e202306849 (2023).
37. Qian, L. et al. Iridium-Catalyzed Enantioselective Transfer Hydrogenation of 1,1-Dialkylethenes with Ethanol: Scope and Mechanism. *J. Am. Chem. Soc.* **146**, 3427–3437 (2024).
38. Zuo, W., Lough, A. J., Li, Y. F. & Morris, R. H. Amine(imine)diphosphine Iron Catalysts for Asymmetric Transfer Hydrogenation of Ketones and Imines. *Science* **342**, 1080–1083 (2013).
39. Pac, C., Ihama, M., Yasuda, M., Miyauchi, Y. & Sakurai, H. Tris(2,2′-Bipyridine)Ruthenium(2 +)-Mediated Photoreduction of Olefins with 1-Benzyl-1,4-Dihydronicotinamide: a Mechanistic Probe for Electron-Transfer Reactions of NAD(P)H-Model Compounds. *J. Am. Chem. Soc.* **103**, 6495–6497 (1981).
40. Kang, W.-J. et al. Discovery of a Thioxanthone-TfOH Complex as a Photoredox Catalyst for Hydrogenation of Alkenes Using p-Xylene as both Electron and Hydrogen Sources. *Angew. Chem. Int. Ed.* **61**, e202211562 (2022).
41. Czyz, M. L., Taylor, M. S., Horngren, T. H. & Polyzos, A. Reductive Activation and Hydrofunctionalization of Olefins by Multiphoton Tandem Photoredox Catalysis. *ACS Catal* **11**, 5472–5480 (2021).

42. Larionova, N. A., Ondozabal, J. M. & Cambeiro, X. C. Reduction of Electron-Deficient Alkenes Enabled by a Photoinduced Hydrogen Atom Transfer. *Adv. Synth. Catal.* **363**, 558–564 (2021).
43. Park, Y. et al. Visible-Light-Driven, Iridium-Catalyzed Hydrogen Atom Transfer: Mechanistic Studies, Identification of Intermediates, and Catalyst Improvements. *JACS Au* **2**, 407–418 (2022).
44. Zhou, W., Dmitriev, I. A. & Melchiorre, P. Reductive Cross-Coupling of Olefins via a Radical Pathway. *J. Am. Chem. Soc.* **145**, 25098–25102 (2023).
45. Schreier, M. R., Pfund, B., Guo, X. & Wenger, O. S. Phototriggered hydrogen atom transfer from an iridium hydride complex to unactivated olefins. *Chem. Sci.* **11**, 8582–8594 (2020).
46. Zhang, J., Mück-Lichtenfeld, C. & Studer, A. Photocatalytic Phosphine-Mediated Water Activation for Radical Hydrogenation. *Nature* **619**, 506–513 (2023).
47. Luo, Y. R. Comprehensive Handbook of Chemical Bond Energies; CRC Press: Boca Raton, FL, (2007).
48. Jeffrey, J. L., Terrett, J. A. & MacMillan, D. W. C. O-H Hydrogen Bonding Promotes H-Atom Transfer from C – H Bonds for C-Alkylation of Alcohols. *Science* **349**, 1532–1536 (2015).
49. Fan, X. et al. Eosin Y as a Direct Hydrogen-Atom Transfer Photocatalyst for the Functionalization of C – H Bonds. *Angew. Chem. Int. Ed.* **57**, 8514–8518 (2018).
50. Liu, L., Liu, J., Liang, X.-A., Wang, S. & Lei, A. Visible Light-Induced Direct α-C – H Functionalization of Alcohols. *Nat. Commun.* **10**, 467–453 (2019).
51. Paul, S. et al. Oxetane Synthesis via Alcohol C – H Functionalization. *J. Am. Chem. Soc.* **145**, 15688–15694 (2023).
52. Twilton, J. et al. Selective Hydrogen Atom Abstraction through Induced Bond Polarization: Direct α-Arylation of Alcohols through Photoredox, HAT, and Nickel Catalysis. *Angew. Chem. Int. Ed.* **57**, 5369–5373 (2018).
53. Capaldo, L., Merli, D., Fagnoni, M. & Ravelli, D. Visible Light Uranyl Photocatalysis: Direct C – H to C – C Bond Conversion. *ACS Catal* **9**, 3054–3058 (2019).
54. Wang, S.-S. & Yang, G.-Y. Recent Advances in Polyoxometalate-Catalyzed Reactions. *Chem. Rev.* **115**, 4893–4962 (2015).
55. Zhang, M. et al. Highly Selective Hydrogenolysis of Lignin B-O-4 Models by A Coupled Polyoxometalate/Cds Photocatalytic System. *Green Chem* **25**, 10091–10100 (2023).
56. Li, S. et al. Hydrogenation Catalysis by Hydrogen Spillover on Platinum-Functionalized Heterogeneous Boronic Acid-Polyoxometalates. *Angew. Chem. Int. Ed.* **62**, e202314999 (2023).
57. Gobbi, A. & Frenking, G. Resonance Stabilization in Allyl Cation, Radical, and Anion. *J. Am. Chem. Soc.* **116**, 9275–9286 (1994).
58. Mo, Y., Lin, Z., Wu, W. & Zhang, Q. Delocalization in Allyl Cation, Radical, and Anion. *J. Phys. Chem.* **100**, 6469–6474 (1996).
59. Hioe, J. & Zipse, H. Radical Stability and Its Role in Synthesis and Catalysis. *Org. Biomol. Chem.* **8**, 3609–3617 (2010).
60. Duncan, D. C., Netzel, T. L. & Hill, C. L. Early-Time Dynamics and Reactivity of Polyoxometalate Excited States. Identification of a Short-Lived LMCT Excited State and a Reactive Long-Lived Charge-Transfer Intermediate Following Picosecond Flash Excitation of $[W_{10}O_{32}]^{4-}$ in Acetonitrile. *Inorg. Chem.* **34**, 4640–4646 (1995).
61. Tanielian, C., Duffy, K. & Jones, A. Kinetic and Mechanistic Aspects of Photocatalysis by Polyoxotungstates: A Laser Flash Photolysis, Pulse Radiolysis, and Continuous Photolysis Study. *J. Phys. Chem. B* **101**, 4276–4282 (1997).
62. Tanielian, C. Decatungstate Photocatalysis. *Coord. Chem. Rev* **178–180**, 1165–1181 (1998).
63. Laudadio, G. et al. C(sp^3)-H Functionalizations of Light Hydrocarbons Using Decatungstate Photocatalysis in Flow. *Science* **369**, 92–96 (2020).
64. Ravelli, D., Fagnoni, M., Fukuyama, T., Nishikawa, T. & Ryu, I. Site-Selective C – H Functionalization by Decatungstate Anion Photocatalysis: Synergistic Control by Polar and Steric Effects Expands the Reaction Scope. *ACS Catal* **8**, 701–713 (2018).
65. De Waele, V., Poizat, O., Fagnoni, M., Bagno, A. & Ravelli, D. Unraveling the Key Features of the Reactive State of Decatungstate Anion in Hydrogen Atom Transfer (HAT) Photocatalysis. *ACS Catal* **6**, 7174–7182 (2016).

Acknowledgements

This work is supported by the Ministry of Education Singapore, AcRF Tier 1 (RG8/25) and A*STAR MTC Individual Research Grants (M21K2c0117) for the financial support (C.-W.S.). Z.-F.Z. and M.-D.S. acknowledge the National Center for High-Performance Computing of Taiwan for generous amounts of computing time and the Ministry of Science and Technology of Taiwan for the financial support.

Author contributions

T.Z., Y.R. Chi, L. Wu, and C.-W.S. conceived and designed the project. T.Z., X.L. and S.-Y.L. performed and analyzed the chemical experiments. Z.-F.Z. and M.-D. S. performed and analyzed the DFT calculations. T.Z., L.Wu, and C.-W.S. analyzed the data and prepared the manuscript. All the authors reviewed the manuscript.

Competing interests

The authors declare no competing interests.

Additional information

Supplementary information The online version contains supplementary material available at https://doi.org/10.1038/s41467-025-67482-1.

Correspondence and requests for materials should be addressed to Ming-Der Su, Yonggui Robin Chi or Cheuk-Wai So.

Peer review information *Nature Communications* thanks Hui Li, and the other, anonymous, reviewers for their contribution to the peer review of this work. A peer review file is available.